A Phosphoproteomic Analysis of the ErbB2 Receptor Tyrosine Kinase Signaling Pathways†

Mridul Mukherji,‡ Laurence M. Brill,§ Scott B. Ficarro,§ Garret M. Hampton,*,§,|| and Peter G. Schultz*,‡,§

Department of Chemistry and The Skaggs Institute for Chemical Biology, The Scripps Research Institute, 10550 North Torrey Pines Road, La Jolla, California 92037, and Genomics Institute of the Novartis Research Foundation, 10675 John Jay Hopkins Drive, San Diego, California 92121

Received May 16, 2006; Revised Manuscript Received September 28, 2006

ABSTRACT: Overexpression of the ErbB2 receptor tyrosine kinase is common in human cancers and is associated with an increased level of metastasis. To better understand the cellular signaling networks activated by ErbB2, a phosphoproteomic analysis of tyrosine-phosphorylated proteins was carried out in ErbB2-overexpressing breast and ovarian cancer cell lines. A total of 153 phosphorylation sites were assigned on 78 proteins. Treatment of cells with Herceptin, a monoclonal antibody that inhibits ErbB2 activity, significantly reduced the number of detectable protein phosphorylation sites, suggesting that many of these proteins participate in ErbB2-driven cell signaling. Of the 71 proteins that were differentially phosphorylated, only 13 were previously reported to directly associate with ErbB2. The differentially phosphorylated proteins included kinases, adaptor/docking proteins, proteins involved in cell proliferation and migration, and several uncharacterized RNA binding proteins. Selective depletion of some of these proteins, including RNA binding proteins SRRM2, SFRS1, SFRS9, and SFRS10, by siRNAs reduced the rate of migration of ErbB2-overexpressing ovarian cancer cells.

The ErbB/Her (human epidermal growth factor receptor) family of receptor tyrosine kinases (RTKs)[1] consists of ErbB1/EGFR (epidermal growth factor receptor), ErbB2, ErbB3, and ErbB4 (*1*). These RTKs have an extracellular region (comprising four domains), a transmembrane domain, and a cytoplasmic tyrosine kinase domain (*1*−*6*). Binding of a ligand to the extracellular region leads to ErbB receptor homo- and heterodimerization, activation of the tyrosine kinase domain, and autophosphorylation of specific tyrosine residues proximal to the C-terminus of the receptor. Intracellular signaling proteins bind to these phosphorylated residues and initiate downstream signaling cascades. In contrast to the other ErbB receptors, no ligand has been identified for ErbB2. Transactivation of ErbB2 by heterodimerization with other ErbB receptors apparently activates specific pathways depending on the heterodimeric partner and its ligand (*1*).

Although activation of ErbB receptors is normally tightly controlled (*7*), abnormal activation has been associated with cellular hyperproliferation (*8*), a hallmark of cancer. Constitutive activation of ErbB2 due to overexpression is observed in 20−30% of breast carcinomas and is associated with a poor prognosis (*8*, *9*). Overexpression of ErbB2 has also been described in ovarian (*9*) and gastric cancers (*10*) and is frequently associated with overexpression of ErbB1 or ErbB3 receptors. When overexpressed in cells of epithelial origin, ErbB2 can form homodimers and ligand-independent heterodimers that cause cell proliferation (*11*, *12*). Furthermore, the therapeutic benefit of Herceptin, a monoclonal antibody that binds to ErbB2 and inhibits its kinase activity, supports the proposal that constitutive ErbB2 signaling frequently promotes aggressive tumor cell behavior (*8*). Collectively, these observations suggest that aberrant activation of biochemical signals by ErbB2-dependent processes contributes to the development of cancer, but the signaling networks that are involved largely remain unclear (*13*).

Despite its importance, a detailed study of the contribution of ErbB2-mediated signaling to oncogenesis is complicated by the relatively large number of phosphorylation events in tumor cells. To more fully inventory the proteins involved in ErbB2 signaling networks, we have used phosphoproteomic techniques (*14*−*16*) to directly assign phosphorylation sites on tyrosine-phosphorylated proteins in an ovarian cancer cell line (SK-OV-3) and a breast cancer cell line (BT-474) that naturally overexpress ErbB2 (*17*). To evaluate the relevance of these protein phosphorylation sites in constitutive ErbB2 signaling, the cells were also treated with Herceptin and profiled for changes in phosphorylation status. These experiments identified a large number of phosphorylation sites on a wide variety of proteins, including a number of kinases, adaptor/docking proteins, and proteins with src-

† The Skaggs Institute of Chemical Biology and the Genomics Institute of the Novartis Research Foundation supported this work. M.M. is a Skaggs Postdoctoral Fellow.

* To whom correspondence should be addressed. E-mail: ghampton@celgene.com (G.M.H.) and schultz@scripps.edu (P.G.S.).

‡ The Scripps Research Institute.

§ Genomics Institute of the Novartis Research Foundation.

|| Present address: Celgene, 4550 Towne Centre Dr., San Diego, CA 92121.

[1] Abbreviations: RTK, receptor tyrosine kinase; ErbB2/HER2, human epidermal growth factor receptor 2; IP, immunoprecipitation; SH2, src-homology 2; SH3, src-homology 3; RRM, RNA recognition motif; RP, reverse-phase; HPLC, high-pressure liquid chromatography; IMAC, immobilized metal affinity chromatography; nanoESI-MS/MS, nanoflow electrospray ionization tandem mass spectrometry; *m*/*z*, mass to charge ratio.

10.1021/bi060971c CCC: $33.50
Published on Web 12/19/2006

homology 2 (SH2), src-homology 3 (SH3), and RNA binding domains that are modulated primarily by ErbB2 activity. Treatment of cells with siRNAs against a number of RNA binding proteins showed that these proteins play roles in cell migration, a phenotype associated with tumor metastasis.

EXPERIMENTAL PROCEDURES

Cell Culture and Sample Preparation. BT-474 and SK-OV-3 cell lines were obtained from American Type Culture Collection (ATCC, Manassas, VA). Cells were grown in media specified by ATCC at 37 °C and 5% CO_2 (media components were from Sigma Chemical Co., St. Louis, MO). Cells (2×10^9 in 150 mm × 25 mm culture plates, 160 plates/preparation) were cultured to approximately 70−80% confluency and washed with 1× Dulbecco's PBS (Sigma). Cells were sequentially lysed in sets of 10 plates with 4 mL/plate of 1× lysis buffer [50 mM Tris (pH 7.5), 100 mM NaCl, 1% Nonidet P-40, 10% glycerol, 20 μg/mL aprotinin, 20 μg/mL leupeptin, 1 mM Pefabloc, 2 mM Na_3VO_4, 1 mM EDTA, and 10 mM β-glycerophosphate] for 10 min at 4 °C. Lysate was transferred to the next set of 10 plates until all cells had been lysed [solubilization of cellular proteins with *n*-octyl β-D-glucopyranoside (OGP) resulted in protein IPs with a reduced level of contamination from abundant cytoskeleton proteins but was not compatible with the subsequent IMAC procedure]. Cells treated with Herceptin (Genentech Inc., South San Francisco, CA) were also cultured in 160 plates per preparation. For SK-OV-3 cells, 8 μg/mL Herceptin was added in the culture media on the same day as the expansion of the cells to 160 plates, whereas BT-474 cells (which grow more slowly) were first cultured for 2 days following expansion; then the medium was replaced with fresh medium containing 8 μg/mL Herceptin. Thus, approximately equal numbers of cells were analyzed following Herceptin treatment for both cell lines. Cells were cultured in the presence of Herceptin for 2 days and then lysed as described above for untreated cells.

Lysates were centrifuged at 15000*g* for 20 min at 4 °C. The monoclonal anti-phosphotyrosine antibody was used for immunoprecipitation [IP; using PT-66-agarose (Sigma)] by adding 500 μL of resin to the lysate from 2×10^9 cells overnight at 4 °C with rotation. Beads from IP were washed with 30 mL of 1× lysis buffer followed by treatment with 12.5 units of RNase A and 500 units of RNase T1 in 10 mL of 1× lysis buffer for 2 h at 4 °C. The beads were then washed two times in 30 mL of 1× lysis buffer and three times with 30 mL of 20 mM Tris (pH 7.4), 120 mM NaCl (wash buffer) at 4 °C. Proteins were recovered from the beads by washing with 8 M urea, 100 mM NH_4HCO_3 (pH 8.0) for 5 min at 96 °C. The eluant was filtered through a poly(vinylidene difluoride) filter (0.2 μm pores), diluted to 4 M urea with water, and digested with 5 μg of modified trypsin (Promega Biosciences Inc., Madison, WI) overnight at 37 °C.

Methylation of Peptides. Tryptic peptides were converted to methyl esters as described previously (*14*, *15*). Tryptic peptides from approximately 1×10^9 cell equivalents of IP protein (above) were desalted on C18 reverse-phase (RP) peptide macrotrap cartridges (Michrom Bioresources, Auburn, CA), eluted with a 70% acetonitrile/30% water/0.1% acetic acid mixture, dried in a Speed Vac plus (Thermo Savant, Holbrook, NY), and treated with 350 μL of 2 N d_3-methanolic DCl. Methanolic DCl was removed by evaporation, and peptides were reconstituted in 100 μL of 0.1% acetic acid and stored at −80 °C.

Immobilized Metal Affinity Chromatography (IMAC). IMAC was carried out as previously reported (*14*, *15*) with the following modifications (*16*). Briefly, methylated peptides were loaded onto a RP desalting column, washed with 0.1% acetic acid, and eluted from the desalting column onto an Fe^{3+}−IMAC column with a HPLC gradient (from 0 to 70% buffer B over 17 min, buffer A being water with 0.1 M acetic acid and buffer B being acetonitrile with 0.1 M acetic acid). Peptides on the IMAC column were washed with a 25% acetonitrile/75% water/0.1% acetic acid mixture containing 100 mM NaCl, followed by 0.1% acetic acid to deplete nonphosphorylated peptides. Phosphopeptides were eluted from IMAC to RP precolumns with 50 mM Na_2HPO_4 (pH 9.0) and immediately washed with 10 μL of 0.1 M acetic acid.

Liquid Chromatography−Tandem Mass Spectrometry. Phosphopeptides on precolumns were analyzed by nanoflow electrospray ionization tandem mass spectrometry (nanoESI-MS/MS) with an LCQ DECA quadrupole ion trap mass spectrometer (Thermo Electron, Inc., San Jose, CA) as described previously (*16*). Peptides were eluted into the mass spectrometer with a HPLC gradient (from 0 to 70% buffer B over 30 min; buffer B as described above). Initially, the flow rate from the emitter tip was set to approximately 100 nL/min. When peptides began to elute, the flow rate was lowered to approximately 25 nL/min by reducing the HPLC flow rate. The mass spectrometer was programmed to operate as described previously (*16*).

Identification of Phosphorylation Sites. MS/MS spectra were matched to peptide sequences in the National Center for Biotechnology Information or Ensembl human protein databases using SEQUEST (Thermo Electron) (*18*). Search parameters specified a differential modification of +80 Da to serine, threonine, and tyrosine residues (phosphorylation) and a static modification of +17 Da to glutamic acid, aspartic acid residues, and peptide C-termini (deuterated methyl groups). Precursor ion tolerances were 1.5 Da, and fragment ion tolerances were 0.5 Da. All reported phosphopeptide assignments were verified by manual interpretation of spectra. Copies of each of the verified MS/MS spectra are available upon request.

Pathway Analysis Using the Ingenuity Knowledge Base. Network analysis using the Ingenuity Knowledge Base (IKB, Ingenuity Systems, Mountain View, CA) was performed by following the method of ref *19* to identify associations among identified phosphoproteins. Interactions are shown in Figure 3 and in Figure S2 of the Supporting Information.

Western Blot Analysis. The mouse anti-ErbB2 and anti-$p27^{Kip1}$ antibodies were obtained from Calbiochem (La Jolla, CA), and the rabbit anti-SFRS10 antibody was obtained from CeMines, Inc. (Golden, CO). HRP-conjugated donkey anti-mouse and anti-rabbit IgG antibodies were obtained from Sigma. Protein concentrations in the lysates were determined with the BCA kit (Pierce, Rockford, IL). For immunoblot analysis, lysates were resolved on sodium dodecyl sulfate−polyacrylamide gels, transferred to a 0.2 μm nitrocellulose membrane (Invitrogen, Carlsbad, CA), and probed with

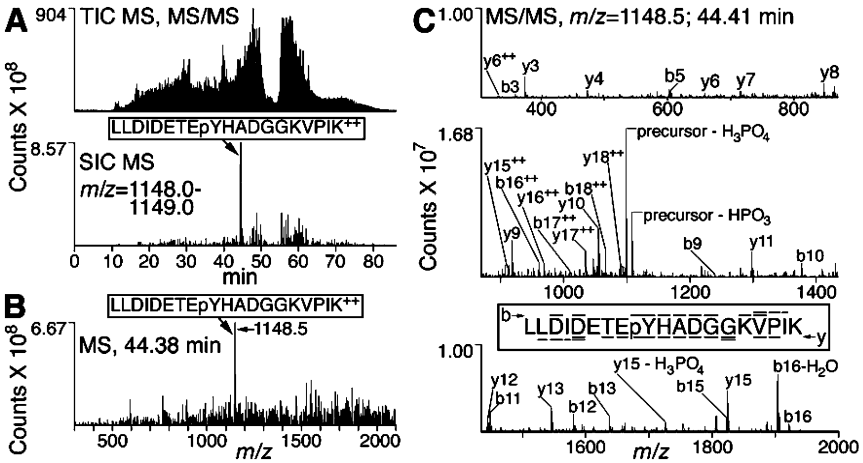

FIGURE 1: NanoLC-MS/MS analyses of ionized phosphopeptides were used to assign protein phosphorylation sites. (A) Total ion chromatogram (TIC, top panel) from an analysis of phosphorylated peptides from SK-OV-3 cells. The selected ion chromatogram (SIC) from the same analysis, showing the ion current with a mass to charge ratio (*m*/*z*) of 1148.0−1149.0, is shown in the bottom panel. The peak representing the $(M + 2H)^{2+}$ ion from the phosphopeptide located in the kinase domain of ErbB2, which contains pY^{877}, was the largest peak in this *m*/*z* range. (B) ESI mass spectrum at 44.38 min showing that the most abundant precursor ion, coinciding with the largest peak from the SIC plot in panel A, had a *m*/*z* of 1148.5. (C) MS/MS spectrum (top, middle, and bottom panels) of the product ions produced by collision-induced dissociation of the precursor ion with a *m*/*z* of 1148.5 (shown in panel B). The b ions (singly and doubly charged) are shown as overlines on the peptide sequence, and the y ions are shown as underlines. These two series of product ions confirmed the ErbB2 peptide sequence and the phosphorylation site at pY^{877}.

indicated antibodies and developed with an ECL+ chemiluminescence kit (Amersham Biosciences, Piscataway, NJ).

siRNA Design. Two siRNAs per gene were designed on the basis of published parameters (*20*). The siRNA oligomers were synthesized by Qiagen Inc. (Valencia, CA) and are listed in Table S1 of the Supporting Information. The siRNA sequences 5′-CUUACGCUGAGUACUUCGA-3′ and 5′-GGUGAUUCACAGAGACAUA-3′ for GL3 firefly luciferase and Aurora-B, respectively, were used as controls.

Quantitative SYBR Green PCR. Cell lysates from SK-OV-3 cells transfected with pooled siRNAs for 3 days were prepared with Trizol (Invitrogen). Total RNA was purified using the RNeasy kit (Qiagen) with on-column DNase digestion of genomic DNA following the manufacturer's protocol. cDNA was prepared from total RNA using the High Capacity cDNA Archive Kit (Applied Biosystems). Quantitative PCRs were carried out with the listed primers (Table S2) using the SYBR Green Master Mix (Applied Biosystems) and monitored on a model 7900HT sequence detection system (Applied Biosystems). For each primer set, standard curves with GL3 siRNA-transfected cDNA were used for quantitation of unknown samples which were calculated using instrument software. Samples were normalized against ribosomal protein L32.

Cell Migration Assay. BT-474 cells grow in clumps and were not suitable for monolayer scratch assays. Therefore, SK-OV-3 cells (4000 cells/well) were transfected with pooled siRNAs for the indicated genes (final concentration of 12.5 nM) using Lipofectamine-2000 (Invitrogen Inc.) in 384-well plates. Two and one-half days after transfection, uniform linear scratches were made on a confluent monolayer of cells using a cell migration assay device (*21*, *22*). After incubation for 6−8 h at 37 °C, the cells were fixed with 4% paraformaldehyde, stained with DAPI, and imaged. Three independent experiments, each containing four replicates, were performed.

Cell Cycle Analysis. Cell cycle analysis following transfection of siRNAs was carried out as previously reported (*23*). Briefly, SK-OV-3 cells (1,500 cells/well; 384 well plate) were transfected with pooled siRNAs for the indicated genes (final concentration of 12.5 nM) using Lipofectamine-2000 (Invitrogen Inc.) in black clear bottom plates. The medium was removed 3 days after transfection; cells were washed with 1× PBS, fixed in 4% paraformaldehyde, and stained with DAPI. Fluorescence intensities of single cells in 384 wells were measured using an imaging cytometer, quantitative three-dimensional microscope (Q3DM, Beckman Coulter Inc., San Diego, CA). The cell cycle profiles were measured using CYTOSHOP (Beckman Coulter Inc.).

RESULTS AND DISCUSSION

Profiling Tyrosine-Phosphorylated Proteins in Tumor Cell Lines Overexpressing ErbB2. To identify phosphoproteins associated with the ErbB2 RTK, tyrosine phosphorylation was profiled in SK-OV-3 and BT-474 cells, which overexpress constitutively active ErbB2 (*17*). Phosphoproteomic analysis of whole cell lysates showed that tyrosine-phosphorylated proteins were present at undetectable levels, and therefore, they were enriched by anti-phosphotyrosine immunoprecipitation (IP). Cells were lysed with NP-40-containing buffer; proteins were fractionated, and the enriched phosphotyrosine proteins were digested with trypsin. The resulting peptide mixtures were treated with d_3-methanolic DCl to esterify free carboxylic acid groups to enhance enrichment of phosphopeptides by immobilized metal affinity chromatography (see Experimental Procedures). Enriched phosphopeptides were eluted via IMAC to RP resin and subjected to nanoESI-MS/MS, and the MS/MS spectra were searched against the human proteome database using SEQUEST (*18*). All peptide sequence matches were manually verified before identification of phosphorylation sites.

These experiments resulted in the assignment of numerous sites of phosphorylation on tyrosine-phosphorylated proteins. Because IP was performed on undigested proteins from whole cell lysates, serine and threonine phosphorylation sites were also assigned on tyrosine-phosphorylated proteins. In addition, phosphorylation sites were

Table 1: Phosphorylation Sites in ErbB2-Overexpressing Breast and Ovarian Cancer Cell Lines[a]

1A

Protein/Gene	Entrez gene Symbol	Entrez gene ID	Y K	S/T K	SH2 dom	PTB dom	SH3 dom	RB dom	Phosporylated Peptide	Phosphorylated Residue(s)	SKOV-3	SK-OV-3 + Hercep	BT-474	BT-474 + Hercep
ErbB2	ERBB2	2064	+						LLDIDETEpYHADGGK	pY877			x	
									LLDIDETEpYHADGGKVPIK	pY877	xxx		xxx	
									FVVIQNEDLGPApSPLDSTFYR	pS998			xx	
									FVVIQNEDLGPASPLDSTFpYR	pY1005			x	
									FVVIQNEDLGPApSPLDSTFpYR	pS998, pY1005			x	
									p(SSSTRS)GGGDLTLGLEPSEEEEAPR	pS1049/1050/1051/1052/1054			xx	
									p(SSSTRS)GGGDLpTLGLEPSEEEEAPR	pS1049/1050/1051/1052/1054, pT1060	xx	x		
									pp(SSSTRS)GGGDLTLGLEPSEEEEAPR	ppS1049/1050/1051/1052/1054	xx	xxx	xxxx	xxxx
									ppp(SSSTRS)GGGDLTLGLEPSEEEAPR	pppS1049/1050/1051/1052/1054		xx		
									HRppp(SSSTRS)GGGDLTLGLEPSEEEEAPR	pppS1049/1050/1051/1052/1054	xxx	xx	xxxxxx	xx
									HRpp(SSSTRS)GGGDLTLGLEPSEEEEAPR	ppS1049/1050/1051/1052/1054	xxx		xxx	x
									HRppp(SSSTRS)GGGDLpTLGLEPSEEEEAPR	pppS1049/1050/1051/1052/1054, pT1060			x	
									pSGGGDLTLGLEPSEEEEAPR	pS1054	x	xxx	xxx	xxx
									pSGGGDLTLGLEPpSEEEAPR	pS1054, pS1066		xxx	x	x
									SPLAPpSEGAGpSDVFDGLGMGAAK	pS1078, pS1083	xx	xxxx	xx	xx
									SPLAPSEGAGpSDVFDGLGMGAAK	pS1083			xxx	
									GLQSLPTHDPpSPLQR	pS1107	xxx	x	xxx	
									PAGApTLER	pT1166	xx	xx		
									PAGApTLERPK	pT1166			xxxxxx	x
									EGPLPAARPAGApTLERPK	pT1166			xx	
									PAGATLERPKpTLpSPGK	pT1172, pS1174			x	
									TLpSPGKNGVVK	pS1174	xx	xx	xxxx	x
									GTPTAENPEpYLGLDVPV	pY1248	x		xx	
EGFR	EGFR	1956	+						MHLPpSPTDSNFYR	pS991	x			
									MHLPSPTDSNFpYR	pY998	x			
									GSHQISLENPEpYQQEFFPK	pY1172	x			
Hepatocyte growth factor receptor	MET	4233	+						DMYDKEpYYSVHNK	pY1234	xx			
AXL receptor tyrosine kinase	AXL	558	+						pYGEVFEPTVER	pY472	x			
									IYNGDpYYR	pY693	xxx			
									IYNGDpYpYRQGR	pY693, pY694	x			
Ephrin receptor EphA2	EPHA2	1969	+						TpYVDPHTpYEDPNQAVLK	pY588, pY594	x		x	
									SEQLKPLKTpYVDPHTpYEDPNQAVLK	pY588, pY594	x		xx	
Ephrin receptor EphB2	EPHB2	2048	+						ADSEpYTDKLQHpYTSGHMTPGMK	pY577, pY584	x			
Ret proto-oncogene	RET	5979	+						RPAQAFPVSpYSSSGAR	pY687			xx	
Inositol 1,4,5-triphosphate receptor	ITPR1	3708							EILIRLpSKLCVQEpSASVR	pS1170, pS1177	x			
Gab1	GAB1	2549							SYpSHDVLPK	pS266	xx		xxxx	
									p(SSS)LEGFHNHFK	pS417/418/419	xxx		xx	
Gads	GRAP2	9402			+		+		pYLQHHHFHQER	pY222			xxx	x
RIP kinase	RIPK1	8737	+	+					LQDEANpYHLYGSR	pY384	xxx			
PI 3-kinase regulatory a-subunit	PIK3R1	5295			+		+		SREYDRLpYEEYTR	pY467	xx			
Erk2	MAPK1	5594		+					VADPDHDHTGFLpTEpYVATR	pT185, pY187	x			
Cdc2	CDC2	983		+					IGEGTpYGVVYK	pY15			x	
Lamin A/C	LMNA	4000							LRLpSPpSPTSQR	pS390, pS392	xx	xx	xx	
									LRLSPpSPTSQR	pS392			x	
Emerin	EMD	2010							GYNDDpYYEESYFTTR	pY94	xx			
TRAP150	THRAP3	9967							IDISPpSTFR	pS684	x			
Interactor Protein Ab1BP4	SSH3BP1	10006					+		NTPpYKTLEPVKPPTVPNDpYMTSPAR	pY198, pY213	x			
SWI/SNF complex 155 kDa subunit	SMARCC1	6599							KHpSPpSPPPPTPTESR	pS328, pS330			xx	xx
Telomerase associated protein TP-1	TEP1	7011							RPPRpSPGMEPPFSHR	pS397	x			
VPARP	ADPRTL1	143							NYDPYKPLDIpTPPPDQK	pT101	x			
									AHpSPASLSFASYR	pS1335	xx			
Pyruvate dehydrogenase	PDHA1	5160							YHGHSMpSDPGVSYR	pS295		x	xx	x
Glyceronephosphate O-acyltransferase	GNPAT	8443							SpSYNLVPR	pS346			x	
NICE-4 protein	NICE-4	9898							RYPSSIp(SSS)PQKDLTQAK	pS607/608/609	xx			
LISCH protein	LISCH7	51599							VLpYYMEK	pY358			x	x
									SRDPHpYDDFR	pY503	xx			

KIAA 0769 protein	SH3MD3	9873			+	SSLYFPRpSPSANEK	pS625	x			
KIAA 1522 protein	KIAA1522	57648				DQpSPPPpSPPPSYHPPPPPTK	pS678, pS682	xxxx			
KIRREL protein	KIRREL	55243				AVLpYADYR	pY311	xx			
						LSHSSGpYAQLNTYSR	pY336	xx			
Hypothetical Protein DKFZp434K1831.1						ARpSQpSPPR	pS32, pS34	x			
Hypothetical Protein LOC144100	LOC144100	144100				KVTpSPLQpSPTK	pS529, pS533	x			
Hypothetical Protein MGC14128	MGC14128	84985				HLYASSKPVMGLKpSPR	pS245	x			
Unnamed protein product	DCBLD1	285761	+			AHTFSAQSGpYRVPGPQPGHK	pY276	xx			
						AHTFSAQSGpYR	pY276			xx	
Totals								67 sites	54 sites	15 sites	33 sites	15 sites
								32 proteins	26 proteins	3 proteins	12 proteins	5 proteins
1B												
Paxillin	PXN	5829				FIHQQPQSSpSPVYGSSAK	pS85	x			
						FIHQQPQSSSPVpYGSSAK	pY88	x	x		
						FIHQQPQSSpSPVpYGSSAK	pS85, pY88	xxxx	xxx	xxxxx	xx
						VGEEEHVpYSFPNKQK	pY118	x			
						VGEEEHVpYSFPNK	pY118	xxx		xxxx	
						VTp(ST)QQQTRIpSASSATR	pS250/pT251, pS258	x			
						DGGRSpSPGGQDEGGFMAQGK	pS303	x			
Focal Adhesion Kinase	PTK2	5747	+			YMEDSpTpYYKASK	pT575, pY576	x			
						YMEDSTpYYKASK	pY576	xx			
						YMEDSTpYYK	pY576	xxx		xx	xx
						YMEDSpp(TYY)KASK	pT575/pY576/pY577	xx			
						THLGTGMERpSPGAMER	pS29	x			
Integrin β-4 chain precursor	ITGB4	3691				MTTTSAAApYGTHLSPHVPHR	pY1469	x			
						MTTTSAAAYGTHLpSPHVPHR	pS1474	x			
						MTTTSAAApYGTHLpSPHVPHR	pY1469, pS1474	x			
α-2 Catenin (CTN2)	CTNNA1	1495				SRTpSVQpTEDDQLIAGQSAR	pS655, pT658			xxxx	
Catenin δ-1, p120 catenin, p120Cas	CTNND1	1500				HYEDGYPGGSDNpYGSLSR	pY228	x		x	
						pYRPSMEGYR	pY241			xxx	
						YRPSMEGpYR	pY248			x	x
Crk-associated substrate p130Cas	BCAR1	9564			+	HLLAPGPQDIpYDVPPVR	pY249	x			
						GLPPSNHHAVpYDVPPSVSK	pY306	x			
						RPGPGTLpYDVPR	pY387	xxx			
Cas-L	NEDD9	4739			+	TGHGYVpYEYPSR	pY166			xxxxx	
Nsp2	BCAR3	8412		+		LpSLTMGGVQAR	pS290	xx			
						RLpSLTMGGVQAR	pS290	x			
SH2-containing protein Nsp1	SH2D3A	10045	+	+		KWpSNSQPADLAHMGR	pS145	x			
Plakophilin 4	PKP4	8502				VApSPSQGQVGSpSSPKR	pS327, pS336	xx			x
Rho guanine nucleotide exchange factor 10	ARHGEF10	9639				SDLp(SSS)SGpSLSLSHGSSSLEHR	pS1034/1035/1036, pS1039	x			
Rac/Cdc42 guanine exchange factor 6	ARHGEF6	9459			+	MpSGFIYQGK	pS32	xx		xx	
Activated p21cdc42Hs kinase	ACK1	10188	+		+	ALPQNDDHpYVMQEHR	pY284	xxx			
						VSSTHpYYLLPERPSYLER	pY857	xxx			
						pYATPQVIQAPGPR	pY234	x		x	
Gene 33/Mig-6	MIG-6	54206				SHpSGPAGSFNKPAIR	pS251	xx	x		
						RSHpSGPAGSFNKPAIR	pS251	x			
Centaurin δ-2 isoform b	CENTD2	116985				RpSFDLpTTPYR	pS257, pT261	x			
Microtubule-associated protein 1B	MAP1B	4131				HMDPPPAPVQDRpSPpSPR	pS2209, pS2211	x			
Drebrin	DBN1	1627				LSpSPVLHR	pS142			xx	
Tensin	TNS	7145		+	+	TVGTNpTPPpSPGFGWR	pT1189, pS1192	x			
FER tyrosine kinase	FER	2241	+	+		pSGVVLLNPIPK	pS542	x			
Caveolin	CAV1	857				pYVDSEGHLYTVPIR	pY6	x			
						YVDSEGHLpYTVPIR	pY14	xx			
						pYVDSEGHLpYTVPIR	pY6, pY14	xx			
LPP	LPP	4026				p(YY)EGYYAAGPGYGGR	pY296/297	xx		x	
						YYEGYpYAAGPGYGGR	pY301	xx		xxx	

Table 1: (Continued)

Protein/Gene	Entrez gene Symbol	Entrez gene ID	Y K	S/T K	SH2 dom	PTB dom	SH3 dom	RB dom	Phosporylated Peptide	Phosphorylated Residue(s)	SKOV-3	SK-OV-3 + Hercep	BT-474	BT-474 + Hercep
Cortactin	EMS1	2017					+		AKTQpTPPVpSPAPQPTEER	pT364, pS368	xx			x
									TQpTPPVpSPAPQPTEER	pT364, pS368	xxx	xxx	xxxx	x
AF6 protein	MLLT4	4301							ADHRp(SS)PNVANQPPpSPGGK	pS1156/1157, pS1166	xxx	x		xx
									EpYFTFPASK	pY1214	x			x
Tight junction protein ZO-2 isoform C	TJP2	9414							AYpSPEYR	pS243			xx	
Coiled-coil protein BICD-2	BICD2	23299							RpSPILLPK	pS582	x			
									GRRpSPILLPK	pS582	xx			
Totals										51 sites	44 sites	7 sites	18 sites	11 sites
										25 proteins	21 proteins	4 proteins	11 proteins	6 proteins
1C														
arginine/serine-rich 1	SFRS1	6426						+	VDGPRpSPSYGR	pS199	x		xx	
									VKVDGPRpSPSYGR	pS199	x			
									VKVDGPRpSPpSYGR	pS199, pS201	x			
									VDGPRpSPSYGRpSR	pS199, pS205	x			
arginine/serine-rich 7	SFRS7	6432						+	YFQSPpSR	pS194	x			
arginine/serine-rich 9	SFRS9	8683						+	STSpYGYSR	pY190	xx		x	
									GpSPHYFSPFRPY	pS211	xxxx			
arginine/serine-rich 10	SFRS10	6434						+	RPHpTPTPGIYMGR	pT201	x			
									RRpSPSPpYYSR	pS264, pY268	xx			
Similar to serine-arginine repetitive matrix 1	SRRM1	10250						+	HRPpSPPApTPPPK	pS402, pT406			x	x
RNA binding region containing 2	RNPC2	9584						+	YRpSPYSGPK	pS97	x			
RNA binding motif protein 3	RBM3	5935						+	p(YY)DSRPGGYGYGYGR	pY117/118	xxxx	x	xxx	
									YYDSRPGGYGpYGYGR	pY127	xx		xx	
Cold inducible RNA binding protein	CIRBP	1153						+	SGGYGGSRDpYYSSR	pY141	xx			
RNA binding motif protein 14	RBM14	10432						+	QPpTPPFFGR	pT206	xxx		xxx	
									DRpSPLRRpSPPR	pS215, pS220	x			
									SPLRRpSPPR	pS220	x			
hnRNP A3	hnRNPA3	10151						+	p(SSGS)PYGGGYGSGGGSGGYGSR	pS356/357/359	xxxx	x	xxxxxx	
hnRPH1	HNRPH1	3187						+	HTGPNpSPDTANDGFVR	pS104	xx			
RNA binding protein 10	RBM10	8241						+	HRHpSPTGPPGFPR	pS89	x		xx	
RNA binding protein	SRRM2	23524						+	THTTALAGRpSPpSPASGR	pS85, pS87	x		xx	x
U1 snRNP 70 kDa	SNRP70	6625						+	YDERPGPpSPLPHR	pS226	x		xx	
Autoantigen p542	RALY	22913						+	GRLpSPVPVPR	pS119	x			
Ribonuclease III, RNase III, p241	RNASE3L	29102						+	HLPPpYPLPK	pY210			xxxx	
Acidic ribosomal phosphoprotein P2	RPLP2	6181						+	KEEpSEEpSDDDMGFGLFD	pS101, pS104		xx	xxx	
Ribosomal protein L23A	RPL23A	6147						+	IRTSPpTFR	pT45	x			
DGCR-8 protein	DGCR8	54487						+	YGGDpSDHPpSDGETSVQPMMTK	pS271, pS275	x			
E1B-55kDa-associated protein 5	E1B-AP5	11100						+	APQQQPPPQQPPPPQPPPQQPPPPPSpYSPAR	pY717	x			
									NYILDQNYGpSAQR	pS512	x			
KIAA 0731 protein	LARP	23367						+	TPRpTPRpTPQLK	pT785, pT788	x			
Totals										35 sites	30 sites	4 sites	15 sites	4 sites
										21 proteins	18 proteins	3 proteins	11 proteins	2 proteins

[a] Individual columns indicate the cell line and, where indicated, treatment with Herceptin (Hercep): Y K, tyrosine kinase; S/T K, serine/threonine kinase; RB, RNA-binding. An x shows that the MS/MS spectrum of the phosphopeptide was identified using SEQUEST followed by manual interpretation in an IMAC-LC−MS/MS analysis. A total of 153 phosphorylation sites were assigned on 78 proteins in this study. Of these 78 phosphoproteins, 13 proteins [EGFR (*39*), GRAP2 (*29*), PIK3R1 (*40*), MAPK1 (*41*), CDC2 (*24*), PXN (*42*), PTK2 (*43*), ITGB4 (*44*), BCAR3 (*29*), SH2D3A (*29*), MIG-6 (*45*), MAP1B (*46*), and FER (*29*)] directly interact with or are phosphorylated by ErbB2. Phosphorylation sites of (A) RTKs, adaptor, regulatory, and unknown proteins, (B) proteins involved in cell migration and cytoskeletal rearrangement, and (C) proteins involved in RNA metabolism. The phosphoproteins common to both cell lines are in bold.

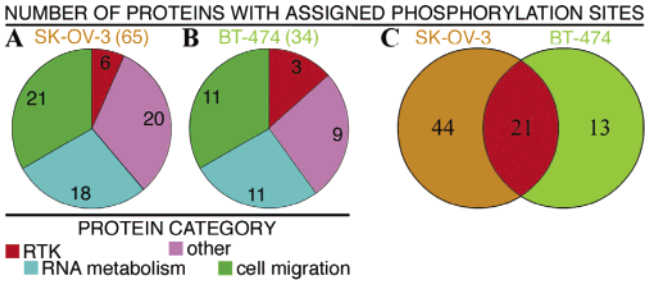

FIGURE 2: Most phosphoproteins from the ErbB2-overexpressing cancer cell lines were in functional classes. Some were detected in a single cell line, whereas others were shared. The number of proteins from the (A) SK-OV-3 and (B) BT-474 cell lines with known or putative functions is shown. The total number of phosphoproteins detected in each cell line is shown in parentheses. (C) Venn diagram indicating the number of unique or overlapping phosphoproteins in or between the two cell lines.

assigned on other proteins that co-immunoprecipitated with the tyrosine-phosphorylated proteins. We repeated experiments at least five times for both cell lines to obtain a comprehensive survey of detectable protein phosphorylation sites and to examine how frequently phosphorylation sites were assigned. As an example, the data that were used to assign a phosphorylation site in the kinase domain of ErbB2, phosphotyrosine 877 (designated pY^{877}), are shown in Figure 1. A total of 153 phosphorylation sites were identified on 78 proteins from the two cancer cell lines (Table 1). The SK-OV-3 cells contained a larger number of proteins with assigned phosphorylation sites (65 proteins, 128 sites) than the BT-474 cell line (34 proteins, 66 sites). These phosphoproteins can be grouped into categories that include RTKs, adaptor/docking proteins, proteins containing SH2 and/or SH3 domains, proteins primarily associated with the regulation of cell migration and RNA metabolism, and novel

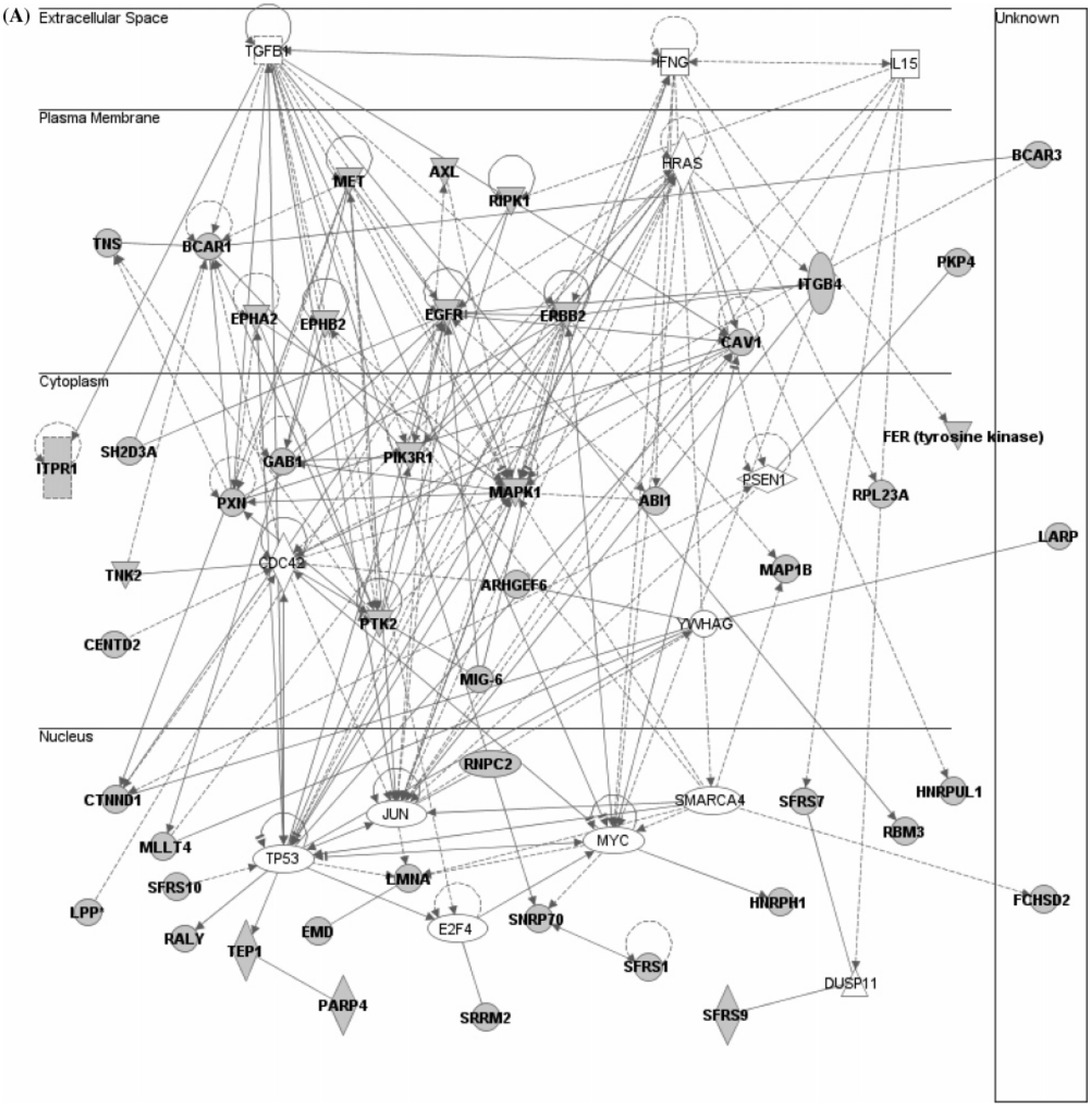

FIGURE 3: Pathway analysis using the Ingenuity Knowledge Base in SK-OV-3 cells. (A) Relationships among phosphoproteins identified in SK-OV-3 cells in the absence of Herceptin.

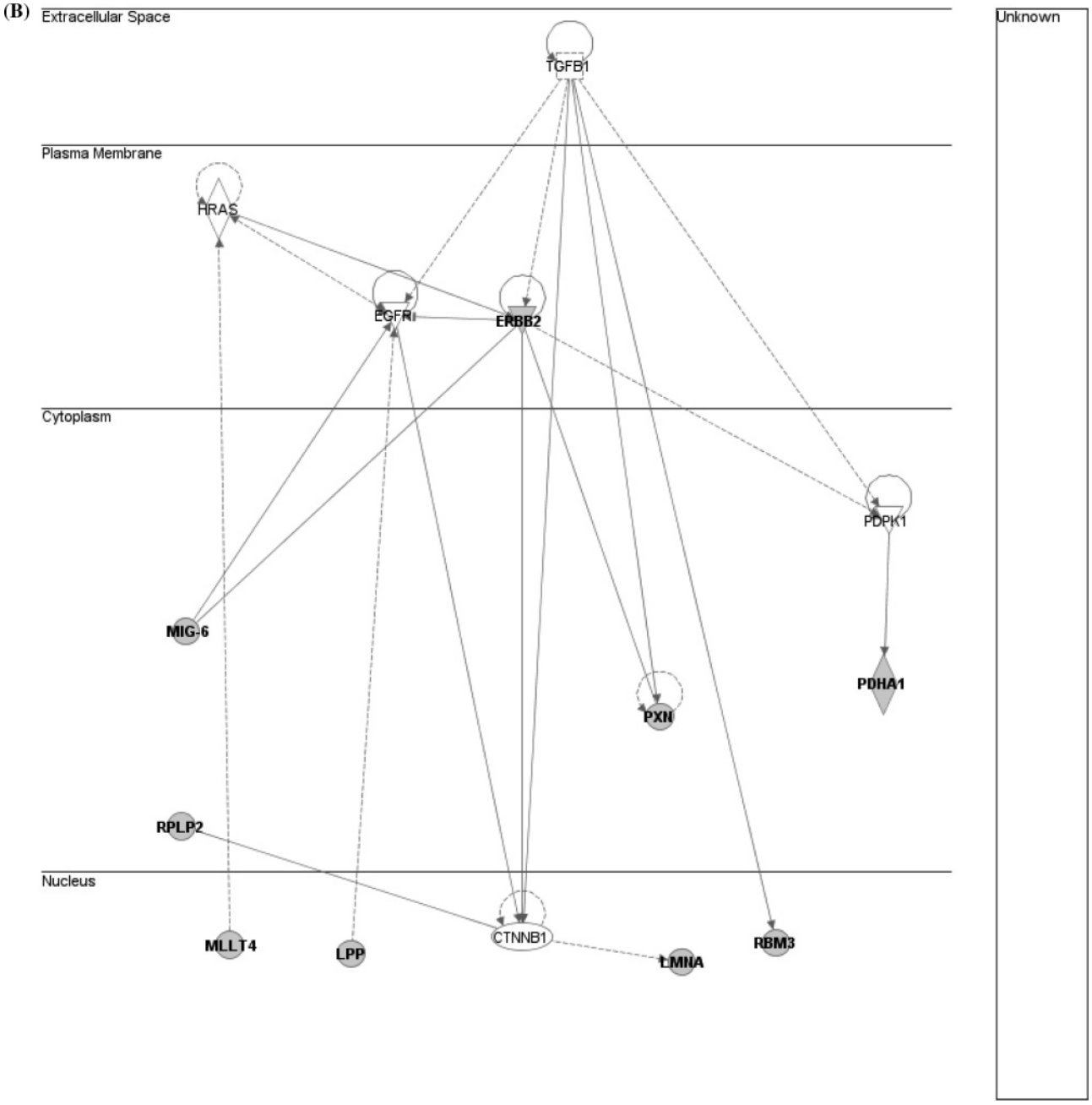

FIGURE 3: (B) Relationships among phosphoproteins identified in SK-OV-3 cells following Herceptin treatment for 2 days. The proteins with a gray background were identified in this study, while proteins with a white background are additional participants in the signaling network. For protein symbols please see Supplemental Figure S2.

proteins (Table 1 and Figure 2A,B). Of the 78 phosphoproteins identified, 21 proteins (including ErbB2) were common to both cell lines (Figure 2C). The remaining 57 phosphoproteins were unique to either the SK-OV-3 or BT-474 cell line. For example, phosphorylation sites on some important signaling proteins were consistently assigned in the breast cancer (BT-474) cell line, but not in the ovarian cancer (SK-OV-3) cell line (Table 1). These proteins include Cdk1/Cdc2 [ErbB2 directly phosphorylates Cdc2 on tyrosine 15 in breast cancer cells (*24*)], human enhancer of filamentation-1 (Hef1/Cas-L), and Grb2-related adaptor protein 2 (Gads).

Effect of Herceptin Treatment on Protein Phosphorylation. To confirm that the identified phosphoproteins participate in ErbB2-mediated signaling, both cell lines were treated with Herceptin and profiled for proteins that are differentially phosphorylated in the presence and absence of Herceptin. Herceptin is a monoclonal antibody that binds to the extracellular domain of ErbB2 and inhibits its kinase activity, leading to rapid dephosphorylation of ErbB2 and inhibition of downstream signal transduction pathways (*5*, *8*). The effects of Herceptin on ErbB2-overexpressing cells were examined by monitoring the accumulation of the $p27^{Kip1}$ protein, an important mediator of ErbB2 signaling (*25*). Treatment of cells with Herceptin did not significantly change the cellular level of ErbB2 protein (Figure S1A,B), whereas an increased level of accumulation of $p27^{Kip1}$ was observed (Figure S1C,D). Accumulation of $p27^{Kip1}$ in both cell lines reached a maximum level after Herceptin treatment for approximately 2 days, and therefore, changes in protein phosphorylation were monitored after Herceptin treatment for 2 days.

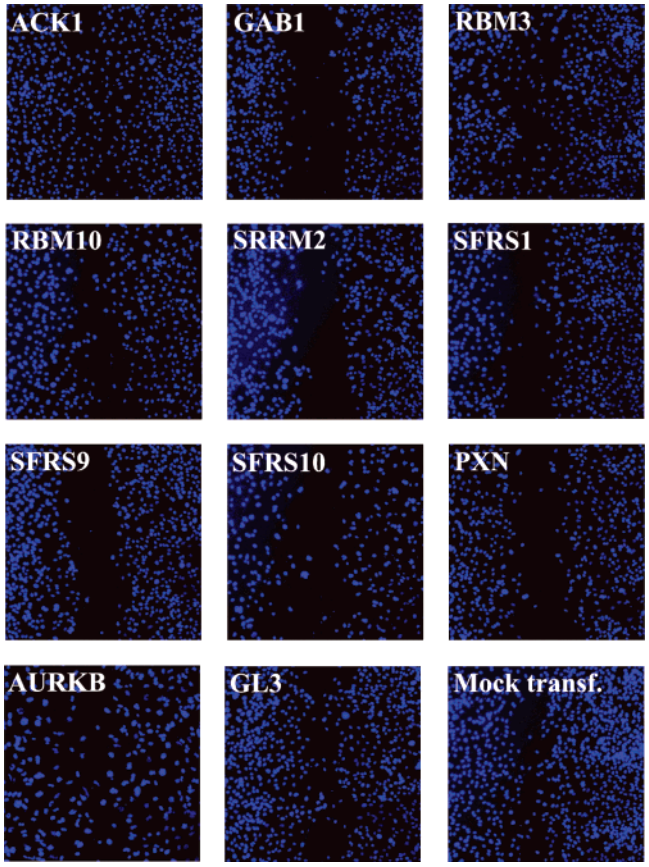

FIGURE 4: RNAi-mediated diminution of genes encoding RNA-binding proteins impedes cell migration. SK-OV-3 cells (4000 cells/well; 384-well plate), transfected with pooled siRNAs for the indicated genes using Lipofectamine-2000, were grown for two and one-half days to develop a confluent monolayer. The monolayer of cells was scratched as described in Experimental Procedures. Six hours after scratching was carried out, the cells were fixed; DNA was stained with DAPI and examined under a fluorescence microscope. Transfection of siRNAs for a number of proteins retarded the migration of SK-OV-3 cells as compared to mock transfection (Mock transf.) and a negative control (GL3). Note that the siRNA for Aurora kinase-B (AURKB), which caused strong cell division arrest, did not inhibit migration of SK-OV-3 cells.

Treatment with Herceptin significantly reduced the number of assigned phosphorylation sites in both SK-OV-3 cells (10 proteins containing 26 phosphorylation sites) and BT-474 cells (13 proteins containing 30 phosphorylation sites) (Table 1). We did not observe tyrosine phosphorylation in any RTKs in either cell line following Herceptin treatment, nor did we observe phosphorylation of the GAB1 adaptor protein, which is a key mediator of signaling initiated by the ErbB2 RTK (*26*). Moreover, in the case of those proteins for which phosphorylation sites could be assigned upon treatment with Herceptin, most had a reduced number of detectable sites (Table 1). For example, the degree of phosphorylation of paxillin, FAK/PTK2, and most RNA binding proteins was significantly reduced by Herceptin treatment. Network analysis using the Ingenuity Knowledge Base with the proteins identified in the presence and absence of Herceptin (Figures 3 and S2) further suggests that the majority of the differentially phosphorylated proteins are members of signaling cascades downstream of ErbB2.

Differential Phosphorylation of Receptor Tyrosine Kinases and Associated Signaling Proteins. Binding of ligand to RTKs leads to autophosphorylation of tyrosine residues on the cytoplasmic domain of the receptor (*27*). These phosphorylation sites serve as foci for the assembly of signaling protein complexes through protein-protein interactions, leading to activation of downstream signaling cascades. In this study Herceptin sensitive tyrosine phosphorylation sites were assigned to six different RTKs (ErbB2, EGFR, Met, Axl, EphA2, and EphB2) in SK-OV-3 cells (Figure 3A) and to three in BT-474 cells (ErbB2, Ret, and EphA2) (Figure S2A and Table 1A), suggesting that distinct, but overlapping, signaling pathways are activated in these ErbB2-overexpressing cancer cell lines. Herceptin sensitive phosphorylation sites were also assigned to key proteins interacting with these RTKs, including multisubstrate adaptor, Grb2-associated binding protein 1 (GAB1) (*26*), which was phosphorylated in both cell lines. GAB1 activates Erk2 mitogen-activated protein kinase (MAPK) by the phosphatidylinositol 3 kinase (PI3K) pathway (*28*); phosphorylation sites were assigned to both the p85 subunit of PI3K and the activation loop of Erk2 in SK-OV-3 cells (Table 1A). In addition, Herceptin sensitive phosphorylation sites were assigned to six proteins with SH2 domains (GRAP2, BCAR3, FER, SH2D3A, TNS, and PIK3R1; five in SK-OV-3 cells and one in BT-474 cells) and nine proteins with SH3 domains (GRAP2, PIK3R1, SSH3BP1, SH3MD3, BCAR1, NEDD9, SH2D3A, ARHGEF6, ACK1, and LPP; eight in SK-OV-3 cells and four in BT-474 cells), consistent with the large number of protein interactions involved in signaling through ErbB2 RTK activation. Indeed, a recent study showed that the SH2 domains of five of these six proteins (GRAP2, BCAR3, FER, SH2D3A, and PIK3R1) directly interact with tyrosine-phosphorylated ErbB2 peptides (*29*).

Differential Phosphorylation of Proteins Involved in Cell Adhesion and Migration. Overall, 51 phosphorylation sites were assigned on 25 proteins (43 phosphorylation sites on 20 proteins were Herceptin sensitive) associated with cell migration and formation of focal adhesion complexes (Table 1B), of which 18 phosphorylation sites on nine proteins were common to both cell lines. Pathway analysis suggests that ErbB2 plays a significant role in controlling cell migration in both cell lines (Figures 3A and S2A). These analyses allow mapping of a cascade of phosphorylation events in the initiation of cell migration and actin reorganization by growth factor and integrin signaling. For example, phosphorylation of RTKs and integrins [two phosphorylation sites were assigned to integrin β4 in SK-OV-3 cells (Table 1B)] results in the recruitment of paxillin (Figure 3A). Paxillin [five Herceptin sensitive phosphorylation sites in SK-OV-3 cells and three Herceptin sensitive phosphorylation sites in BT474 cells (Table 1B)] serves as a central docking protein for recruitment of many signaling proteins to focal adhesions, including tyrosine kinases FAK [four Herceptin sensitive phosphorylation sites assigned to SK-OV-3 cells and one Herceptin unsensitive site in BT474 cells (Table 1B)], Src, and Abl (*30*). Phosphorylation of paxillin at tyrosine 31 and 118 by FAK and/or Src leads to binding of Crk family docking proteins (*30*) (Figure 3A). The Crk proteins then bind to phosphorylated BCAR1 (Crk-associated substrate p130Cas) (*31*). Novel phosphorylation sites were assigned to three tyrosine residues in the binding site for Crk-SH2 domains on BCAR1 [pY^{249}, pY^{306}, and pY^{387} in SK-OV-3 cells, all Herceptin sensitive (Table 1B)]. These protein−protein interactions finally lead to activation of cell motility

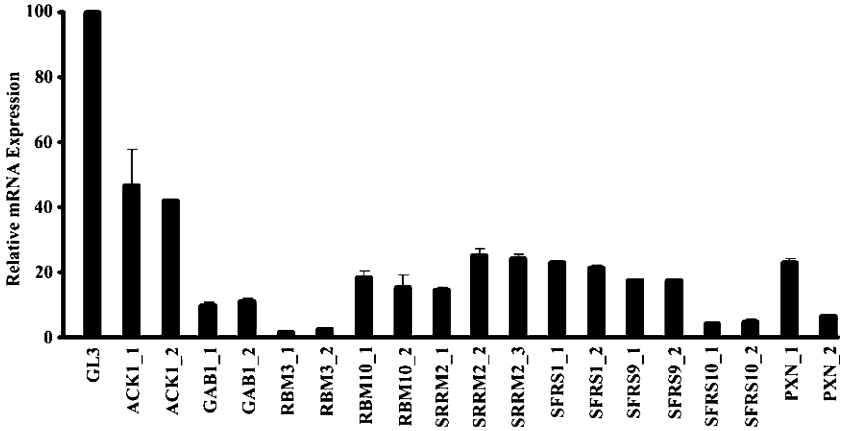

FIGURE 5: Knockdown analysis with siRNAs for selected genes. SK-OV-3 cells (300 000 cells/10 cm dish), transfected with pooled siRNAs for the indicated genes using Lipofectamine-2000, were grown for 3 days before total mRNA isolation using the RNeasy kit. The relative quantities of mRNA remaining after transfection with pooled siRNAs compared to a GL3 siRNA negative control were determined by quantitative PCR using specific primers for each gene. The relative mRNA quantities of genes after GL3 siRNA transfection are shown only once for representation. The indicated values are averages of two qPCR replicates.

signals (Figure 3A). In addition to the identification of novel phosphorylation sites on known proteins, a number of novel phosphoproteins that were identified (Table 1) may also have roles in ErbB2-mediated signaling.

Differential Phosphorylation of RNA Binding Proteins. Our phosphoproteomic analysis identified 35 phosphorylation sites on 21 proteins containing RNA binding domains: 30 sites on 18 proteins in SK-OV-3 cells and 15 sites on 11 proteins in BT-474 cells (Table 1C). The presence of the RNA binding protein SFRS10 in the anti-phosphotyrosine IP from SK-OV-3 cells was confirmed by Western blot analysis using an existing antibody specific for SFRS10 (Figure S3). The identified RNA binding proteins from our analysis included 13 phosphorylation sites on eight Herceptin sensitive proteins (SFRS1, SFRS9, RBM3, RBM14, hnRNPA3, RBM10, SRRM2, and SNRP70) that were common to both cell lines. These proteins were primarily from two families of RNA binding proteins, the SR and hnRNP families. Several studies indicate that cellular signaling pathways can modulate gene expression at the level of mRNA splicing or translation through the actions of RNA binding proteins (*32*, *33*). The reduced number of phosphorylation sites in both ErbB2-overexpressing cell lines following Herceptin treatment [four sites on three proteins in SK-OV-3 cells and four sites on two proteins in BT-474 cells (Table 1C)] suggested that these RNA binding proteins also function downstream of the ErbB2 receptor. However, a role of RNA binding proteins in ErbB2 signaling has not been previously reported.

To determine the biological relevance of these RNA binding proteins in ErbB2 signaling, siRNAs were designed against eight Herceptin sensitive phosphoproteins (Table S1). Of these eight proteins, seven were common to both cell lines and six had RNA binding domains. Two siRNAs per gene were designed on the basis of reported transcripts for these genes and results of the proteomic peptide mapping experiments. SK-OV-3 cells were transfected by pooling the two siRNAs targeting the same gene in 384-well plates and assayed for their ability to affect cell migration, since overexpression of ErbB2 has been associated with metastatic lesions (*34*). A siRNA targeting firefly luciferase (GL3) sequence was used as a negative control, while siRNAs against paxillin (PXN) were used as a positive control. The ability of SK-OV-3 cells to migrate following transfection of the siRNAs was assessed using an image-based assay of cell monolayer wound healing (*21*, *22*). SK-OV-3 cells exhibited significantly retarded migration following transfection with siRNAs targeting five genes (GAB1, SRRM2, SFRS1, SFRS9, and SFRS10) compared to mock transfection (no siRNA) or cells transfected with the negative control GL3 siRNA (Figure 4). Impeded migration of SK-OV-3 cells following transfection of siRNAs for these five genes was comparable to the effect observed following transfection of paxillin siRNAs. Although similar numbers of cells were seeded in every well, transfection of siRNAs targeting the SFRS10 gene reduced the cell density due to a delay in G_2/M phase progression. However, a reduced rate of migration of SK-OV-3 cells following transfection of siRNAs targeting the SFRS10 gene was not due to its effect on the cell cycle, since transfection of SK-OV-3 cells with the siRNA for Aurora-B, which resulted in strong G_2/M arrest (Figure S4), did not significantly inhibit cell migration.

To confirm that the retarded migration of SK-OV-3 cells following transfection of the siRNAs was due to selective depletion of target mRNAs, quantitative PCR (qPCR) was performed. For accurate measurement of target mRNA quantities, at least two primer pairs were selected for each gene for qPCR studies (Table S2), and when possible, these primer pairs flanked the region containing sequences targeted by siRNAs. Quantitative PCR analysis of ACK1 showed moderate depletion of target mRNA (≈50%, Figure 5), suggesting that the lack of an effect of its siRNAs on cell migration (Figure 4) could be due to insufficient knockdown. The siRNAs for the RBM3 and RBM10 genes also did not significantly reduce the rate of cell migration, although they caused strong target mRNA depletion (>70%, Figure 5), suggesting that these genes are not involved in the migration of SK-OV-3 cells. The qPCR experiments for five other genes (GAB1, SRRM2, SFRS1, SFRS9, and SFRS10) that effected cell migration showed strong (>70%) depletion of target mRNAs with two separate primer pairs following transfection of siRNAs when compared with the negative control GL3 transfections under identical conditions (Figure 5). For quantitation of SRRM2 mRNA, three primer pairs were used, and although none of them flanked the siRNA sequences used to target this gene, all three exhibited a

significant knockdown of the target mRNA. These results demonstrate a novel role for RNA binding proteins SRRM2, SFRS1, SFRS9, and SFRS10 in cell migration.

Recently, de Hoog et al. (*33*) using stable isotope labeling in cell culture (SILAC)-based quantitative proteomics techniques showed that tyrosine-phosphorylated RNA binding proteins, primarily of the Sm and hnRNP classes, participate in the initial stages of cell spreading by forming ribonucleoprotein complexes [spreading initiation complex (SIC)] in noncancerous cells. A triple SILAC-based analysis of EGFR signaling identified six RNA binding proteins, four of which were from the hnRNP class, in cancerous HeLa cells (*35*) but did not identify any sites of phosphorylation. In this study, we have identified many novel phosphorylation sites on RNA binding proteins, mainly from the SR and hnRNP classes that act downstream of ErbB2, and a number of these have a role in cell migration. This is an important finding because ErbB2 overexpression is associated with aggressive metastatic (migratory) behavior of tumors (*36*) and thus sheds new light on the mechanism of ErbB2-driven cell signaling.

Finally, a bioinformatics analysis was performed to search for motifs that were over-represented in the phosphoproteins which were identified from ErbB2-overexpressing cells. Overrepresented motifs may predict optimum peptide sequences required for phosphorylation by ErbB2 dependent kinases. This approach recently identified a number of known and novel phosphorylation motifs from large proteomic data sets (*37*). Our analysis identified enrichment of two motifs, YDxPP and Rx_3Yx_3RxR, which were 43- and 18-fold overrepresented, respectively, compared to the complete human proteome (significance = 0.0001) (Table S3). A total of 25 related sequences were identified in 11 phosphoproteins (Table S4): 15 YDxPP motifs in four proteins (GAB1, BCAR1, SH3MD3, and NEDD9) and 10 Rx_3Yx_3RxR motifs in seven proteins (SFRS1, SFRS7, SFRS9, THRAP3, RNASE3L, E1B-AP5, and LISCH7). Most of these phosphoproteins that contained one of the two identified motifs, with the exception of LISCH7, were Herceptin sensitive. The GAB1 and BCAR1 proteins, both containing the YDxPP motif, play essential roles during ErbB2-mediated transformation (*26*) and cell invasion (*38*), respectively. Two of three phosphorylation sites assigned on BCAR1 are within this motif [pY^{249} and pY^{306} (Table 1)]. The Rx_3Yx_3RxR motif was present in a number of RNA binding proteins including SFSR1, SFRS7, SFRS9, RNASE3L, and E1B-AP5. Interestingly, in a study by Schwartz et al., the largest number of novel phosphorylation motifs were identified in proteins involved in RNA binding and splicing (*37*). These results reinforce the notion that RNA binding proteins play an important role in ErbB2 signaling.

ACKNOWLEDGMENT

We thank Stuart Cahalan, Jaimeet Singh Chhabra, Michelle Stettler-Gill, and Eric Peters for data analysis and helpful discussions. This is paper 16534-CH of The Scripps Research Institute.

SUPPORTING INFORMATION AVAILABLE

Western blots showing accumulation of the $p27^{Kip1}$ protein without significant changes in the cellular level of ErbB2 protein following Herceptin treatment and presence of SFRS10 protein in the anti-pY IP, cell cycle analysis showing the increase in the G_2/M population when transfected with the siRNAs for SFRS10 and Aurora-B genes, sequences of siRNAs as well as primers used to quantitate the mRNA levels, and a list of over-represented motifs from identified phosphoproteins. This material is available free of charge via the Internet at http://pubs.acs.org.

REFERENCES

1. Olayioye, M. A., Neve, R. M., Lane, H. A., and Hynes, N. E. (2000) The ErbB signaling network: Receptor heterodimerization in development and cancer, *EMBO J. 19*, 3159−67.
2. Ogiso, H., Ishitani, R., Nureki, O., Fukai, S., Yamanaka, M., Kim, J. H., Saito, K., Sakamoto, A., Inoue, M., Shirouzu, M., and Yokoyama, S. (2002) Crystal structure of the complex of human epidermal growth factor and receptor extracellular domains, *Cell 110*, 775−87.
3. Ferguson, K. M., Berger, M. B., Mendrola, J. M., Cho, H. S., Leahy, D. J., and Lemmon, M. A. (2003) EGF activates its receptor by removing interactions that autoinhibit ectodomain dimerization, *Mol. Cell 11*, 507−17.
4. Cho, H. S., and Leahy, D. J. (2002) Structure of the extracellular region of HER3 reveals an interdomain tether, *Science 297*, 1330−3.
5. Cho, H. S., Mason, K., Ramyar, K. X., Stanley, A. M., Gabelli, S. B., Denney, D. W., Jr., and Leahy, D. J. (2003) Structure of the extracellular region of HER2 alone and in complex with the Herceptin Fab, *Nature 421*, 756−60.
6. Garrett, T. P., McKern, N. M., Lou, M., Elleman, T. C., Adams, T. E., Lovrecz, G. O., Zhu, H. J., Walker, F., Frenkel, M. J., Hoyne, P. A., Jorissen, R. N., Nice, E. C., Burgess, A. W., and Ward, C. W. (2002) Crystal structure of a truncated epidermal growth factor receptor extracellular domain bound to transforming growth factor α, *Cell 110*, 763−73.
7. Vermeer, P. D., Einwalter, L. A., Moninger, T. O., Rokhlina, T., Kern, J. A., Zabner, J., and Welsh, M. J. (2003) Segregation of receptor and ligand regulates activation of epithelial growth factor receptor, *Nature 422*, 322−6.
8. Yarden, Y., and Sliwkowski, M. X. (2001) Untangling the ErbB signalling network, *Nat. Rev. Mol. Cell Biol. 2*, 127−37.
9. Slamon, D. J., Godolphin, W., Jones, L. A., Holt, J. A., Wong, S. G., Keith, D. E., Levin, W. J., Stuart, S. G., Udove, J., Ullrich, A., et al. (1989) Studies of the HER-2/neu proto-oncogene in human breast and ovarian cancer, *Science 244*, 707−12.
10. Yonemura, Y., Ninomiya, I., Yamaguchi, A., Fushida, S., Kimura, H., Ohoyama, S., Miyazaki, I., Endou, Y., Tanaka, M., and Sasaki, T. (1991) Evaluation of immunoreactivity for erbB-2 protein as a marker of poor short term prognosis in gastric cancer, *Cancer Res. 51*, 1034−8.
11. Holbro, T., Beerli, R. R., Maurer, F., Koziczak, M., Barbas, C. F., III, and Hynes, N. E. (2003) The ErbB2/ErbB3 heterodimer functions as an oncogenic unit: ErbB2 requires ErbB3 to drive breast tumor cell proliferation, *Proc. Natl. Acad. Sci. U.S.A. 100*, 8933−8.
12. Muthuswamy, S. K., Li, D., Lelievre, S., Bissell, M. J., and Brugge, J. S. (2001) ErbB2, but not ErbB1, reinitiates proliferation and induces luminal repopulation in epithelial acini, *Nat. Cell Biol. 3*, 785−92.
13. Holbro, T., Civenni, G., and Hynes, N. E. (2003) The ErbB receptors and their role in cancer progression, *Exp. Cell Res. 284*, 99−110.
14. Ficarro, S. B., McCleland, M. L., Stukenberg, P. T., Burke, D. J., Ross, M. M., Shabanowitz, J., Hunt, D. F., and White, F. M. (2002) Phosphoproteome analysis by mass spectrometry and its application to *Saccharomyces cerevisiae*, *Nat. Biotechnol. 20*, 301−5.
15. Salomon, A. R., Ficarro, S. B., Brill, L. M., Brinker, A., Phung, Q. T., Ericson, C., Sauer, K., Brock, A., Horn, D. M., Schultz, P. G., and Peters, E. C. (2003) Profiling of tyrosine phosphorylation pathways in human cells using mass spectrometry, *Proc. Natl. Acad. Sci. U.S.A. 100*, 443−8.
16. Brill, L. M., Salomon, A. R., Ficarro, S. B., Mukherji, M., Stettler-Gill, M., and Peters, E. C. (2004) Robust phosphoproteomic profiling of tyrosine phosphorylation sites from human T cells using immobilized metal affinity chromatography and tandem mass spectrometry, *Anal. Chem. 76*, 2763−72.

17. Lewis, G. D., Figari, I., Fendly, B., Wong, W. L., Carter, P., Gorman, C., and Shepard, H. M. (1993) Differential responses of human tumor cell lines to anti-p185HER2 monoclonal antibodies, *Cancer Immunol. Immunother. 37*, 255−63.
18. Eng, J. K., McCormack, A. L., and Yates, J. R., III (1994) An Approach to Correlate Tandem Mass Spectral Data of Peptides with Amino Acid Sequences in a Protein Database, *J. Am. Soc. Mass Spectrom. 5*, 976−89.
19. Calvano, S. E., Xiao, W., Richards, D. R., Felciano, R. M., Baker, H. V., Cho, R. J., Chen, R. O., Brownstein, B. H., Cobb, J. P., Tschoeke, S. K., Miller-Graziano, C., Moldawer, L. L., Mindrinos, M. N., Davis, R. W., Tompkins, R. G., and Lowry, S. F. (2005) A network-based analysis of systemic inflammation in humans, *Nature 437*, 1032−7.
20. Aza-Blanc, P., Cooper, C. L., Wagner, K., Batalov, S., Deveraux, Q. L., and Cooke, M. P. (2003) Identification of modulators of TRAIL-induced apoptosis via RNAi-based phenotypic screening, *Mol. Cell 12*, 627−37.
21. Yarrow, J. C., Totsukawa, G., Charras, G. T., and Mitchison, T. J. (2005) Screening for cell migration inhibitors via automated microscopy reveals a Rho-kinase inhibitor, *Chem. Biol. 12*, 385−95.
22. Collins, C. S., Hong, J., Sapinoso, L., Zhou, Y., Liu, Z., Micklash, K., Schultz, P. G., and Hampton, G. M. (2006) A small interfering RNA screen for modulators of tumor cell motility identifies MAP4K4 as a promigratory kinase, *Proc. Natl. Acad. Sci. U.S.A. 103*, 3775−80.
23. Mukherji, M., Bell, R., Supekova, L., Wang, Y., Orth, A. P., Batalov, S., Miraglia, L., Huesken, D., Lange, J., Martin, C., Sahasrabudhe, S., Reinhardt, M., Natt, F., Hall, J., Mickanin, C., Labow, M., Chanda, S. K., Cho, C. Y., and Schultz, P. G. (2006) Genome-wide functional analysis of human cell cycle regulators, *Proc. Natl. Acad. Sci. U.S.A. 103*, 14819−14824.
24. Tan, M., Jing, T., Lan, K. H., Neal, C. L., Li, P., Lee, S., Fang, D., Nagata, Y., Liu, J., Arlinghaus, R., Hung, M. C., and Yu, D. (2002) Phosphorylation on tyrosine-15 of p34(Cdc2) by ErbB2 inhibits p34(Cdc2) activation and is involved in resistance to taxol-induced apoptosis, *Mol. Cell 9*, 993−1004.
25. Lane, H. A., Beuvink, I., Motoyama, A. B., Daly, J. M., Neve, R. M., and Hynes, N. E. (2000) ErbB2 potentiates breast tumor proliferation through modulation of p27(Kip1)-Cdk2 complex formation: Receptor overexpression does not determine growth dependency, *Mol. Cell. Biol. 20*, 3210−23.
26. Yamasaki, S., Nishida, K., Yoshida, Y., Itoh, M., Hibi, M., and Hirano, T. (2003) Gab1 is required for EGF receptor signaling and the transformation by activated ErbB2, *Oncogene 22*, 1546−56.
27. Schlessinger, J. (2000) Cell signaling by receptor tyrosine kinases, *Cell 103*, 211−25.
28. Takahashi-Tezuka, M., Yoshida, Y., Fukada, T., Ohtani, T., Yamanaka, Y., Nishida, K., Nakajima, K., Hibi, M., and Hirano, T. (1998) Gab1 acts as an adapter molecule linking the cytokine receptor gp130 to ERK mitogen-activated protein kinase, *Mol. Cell. Biol. 18*, 4109−17.
29. Jones, R. B., Gordus, A., Krall, J. A., and MacBeath, G. (2006) A quantitative protein interaction network for the ErbB receptors using protein microarrays, *Nature 439*, 168−74.
30. Turner, C. E. (2000) Paxillin and focal adhesion signaling, *Nat. Cell Biol. 2*, E231−6.
31. Ruest, P. J., Shin, N. Y., Polte, T. R., Zhang, X., and Hanks, S. K. (2001) Mechanisms of CAS substrate domain tyrosine phosphorylation by FAK and Src, *Mol. Cell. Biol. 21*, 7641−52.
32. Rooke, N., Markovtsov, V., Cagavi, E., and Black, D. L. (2003) Roles for SR proteins and hnRNP A1 in the regulation of c-src exon N1, *Mol. Cell. Biol. 23*, 1874−84.
33. de Hoog, C. L., Foster, L. J., and Mann, M. (2004) RNA and RNA binding proteins participate in early stages of cell spreading through spreading initiation centers, *Cell 117*, 649−62.
34. Eccles, S. A. (2000) Cell biology of lymphatic metastasis. The potential role of c-erbB oncogene signaling, *Recent Results Cancer Res. 157*, 41−54.
35. Blagoev, B., Ong, S. E., Kratchmarova, I., and Mann, M. (2004) Temporal analysis of phosphotyrosine-dependent signaling networks by quantitative proteomics, *Nat. Biotechnol. 22*, 1139−45.
36. Li, Y. M., Pan, Y., Wei, Y., Cheng, X., Zhou, B. P., Tan, M., Zhou, X., Xia, W., Hortobagyi, G. N., Yu, D., and Hung, M. C. (2004) Upregulation of CXCR4 is essential for HER2-mediated tumor metastasis, *Cancer Cell 6*, 459−69.
37. Schwartz, D., and Gygi, S. P. (2005) An iterative statistical approach to the identification of protein phosphorylation motifs from large-scale data sets, *Nat. Biotechnol. 23*, 1391−8.
38. Spencer, K. S., Graus-Porta, D., Leng, J., Hynes, N. E., and Klemke, R. L. (2000) ErbB2 is necessary for induction of carcinoma cell invasion by ErbB family receptor tyrosine kinases, *J. Cell Biol. 148*, 385−97.
39. Kiguchi, K., Bol, D., Carbajal, S., Beltran, L., Moats, S., Chan, K., Jorcano, J., and DiGiovanni, J. (2000) Constitutive expression of erbB2 in epidermis of transgenic mice results in epidermal hyperproliferation and spontaneous skin tumor development, *Oncogene 19*, 4243−54.
40. Ghatak, S., Misra, S., and Toole, B. P. (2005) Hyaluronan constitutively regulates ErbB2 phosphorylation and signaling complex formation in carcinoma cells, *J. Biol. Chem. 280*, 8875−83.
41. Timms, J. F., White, S. L., O'Hare, M. J., and Waterfield, M. D. (2002) Effects of ErbB-2 overexpression on mitogenic signalling and cell cycle progression in human breast luminal epithelial cells, *Oncogene 21*, 6573−86.
42. Fernandez-Valle, C., Tang, Y., Ricard, J., Rodenas-Ruano, A., Taylor, A., Hackler, E., Biggerstaff, J., and Iacovelli, J. (2002) Paxillin binds schwannomin and regulates its density-dependent localization and effect on cell morphology, *Nat. Genet. 31*, 354−62.
43. Vartanian, T., Goodearl, A., Lefebvre, S., Park, S. K., and Fischbach, G. (2000) Neuregulin induces the rapid association of focal adhesion kinase with the erbB2-erbB3 receptor complex in schwann cells, *Biochem. Biophys. Res. Commun. 271*, 414−7.
44. Gambaletta, D., Marchetti, A., Benedetti, L., Mercurio, A. M., Sacchi, A., and Falcioni, R. (2000) Cooperative signaling between $\alpha_6\beta_4$ integrin and ErbB-2 receptor is required to promote phosphatidylinositol 3-kinase-dependent invasion, *J. Biol. Chem. 275*, 10604−10.
45. Fiorentino, L., Pertica, C., Fiorini, M., Talora, C., Crescenzi, M., Castellani, L., Alema, S., Benedetti, P., and Segatto, O. (2000) Inhibition of ErbB-2 mitogenic and transforming activity by RALT, a mitogen-induced signal transducer which binds to the ErbB-2 kinase domain, *Mol. Cell. Biol. 20*, 7735−50.
46. Alaoui-Jamali, M. A., Song, D. J., Benlimame, N., Yen, L., Deng, X., Hernandez-Perez, M., and Wang, T. (2003) Regulation of multiple tumor microenvironment markers by overexpression of single or paired combinations of ErbB receptors, *Cancer Res. 63*, 3764−74.

BI060971C